LIMNOLOGY and OCEANOGRAPHY: METHODS

ASLO

*Limnol. Oceanogr.: Methods* 2022

doi: 10.1002/lom3.10515

# Use of metal oxide semiconductor sensors to measure methane in aquatic ecosystems in the presence of cross-interfering compounds

**Andrea Butturini** [1]*, **Jordi Fonollosa** [2,3,4]

[1]Department de Biologia evolutiva, Ecologia i Ciències Ambientals, Universitat de Barcelona, Barcelona, Catalonia, Spain
[2]B2SLab, Departament d'Enginyeria de Sistemes, Automàtica i Informàtica Industrial, Universitat Politècnica de Catalunya, Barcelona, Spain
[3]Networking Biomedical Research Centre in Bioengineering, Biomaterials and Nanomedicine (CIBER-BBN), Madrid, Spain
[4]Institut de Recerca Sant Joan de Déu, Esplugues de Llobregat, Spain

## Abstract

Monitoring dissolved methane in aquatic ecosystems contributes significantly to advancing our understanding of the carbon cycle in these habitats and capturing their impact on methane emissions. Low-cost metal oxide semiconductors (MOS) gas sensors are becoming an increasingly attractive tool to perform such measurements, especially at the air–water interface. However, the performance of MOS sensors in aquatic environmental sciences has come under scrutiny because of their cross-sensitivity to temperature, moisture, and sulfide interference. In this study, we evaluated the performance and limitations of a MOS methane sensor when measuring dissolved methane in waters. A MOS sensor was encapsulated in a hydrophobic extended polytetrafluoroethylene membrane to impede contact with water but allow gas perfusion. Therefore, the membrane enabled us to submerge the sensor in water and overcome cross-sensitivity to humidity. A simple portable, low-energy, flow-through cell system was assembled that included an encapsulated MOS sensor and a temperature sensor. Waters (with or without methane) were injected into the flow cell at a constant rate by a peristaltic pump. The signals from the two sensors were recorded continuously with a cost-efficient microcontroller. Tests specifically focused on the effect of water temperature and sulfide interference on sensor performance. Our experiments revealed that the lower limit of the sensor was in the range of 0.1–0.2 $\mu$mol $L^{-1}$ and that it provided a stable response at water temperatures in the range of 18.5–28°C. Dissolved sulfide at a concentration of 0.4 mmol $L^{-1}$ or higher interfered with the sensor response, especially at low methane concentrations (0.5 $\mu$mol $L^{-1}$ or lower). However, we show that if dissolved sulfide is monitored, its interference can be alleviated.

## Introduction

Methane is a powerful greenhouse gas with a concentration that has increased almost threefold in the industrial era (Saunois et al. 2020). Consequently, the study of its origin, abundance, and consume is now a research priority in the environmental sciences. The availability of small, low-cost methane sensors based on metal oxide semiconductor (MOS) technology is rapidly attracting research attention for the purposes of monitoring methane in air at ambient concentrations (Eugster and Kling 2012; van den Bossche et al. 2017).

Continental aquatic ecosystems, especially shallow water bodies (wetlands, ponds, small lakes) are a significant component of the global carbon budget and biogeochemists are starting to implement MOS technology to study methane fluxes at the water–atmosphere interface (Jørgensen et al. 2020) using floating flux chambers (Bastviken et al. 2020).

Here, we report the possibilities and limitations of using a low-cost device with MOS technology to measure the concentration of methane dissolved in water. Although dissolved methane does not represent the total methane available in aquatic ecosystems (saturation bubbling and ebullition can be substantial fluxes), such a device may prove useful to elucidate uncertainties about methane production and consumption in aquatic ecosystems worldwide. Many researchers have

*Correspondence: abutturini@ub.edu

**Authors Contribution Statement:** A.B. conceived the study and conducted the experiments. J.F. set up the electronics and performed the data analysis. A.B. and J.F. wrote and revised the manuscript and planned the schemes, figures, and tables.

Additional Supporting Information may be found in the online version of this article.

attempted to estimate global methane emissions from inland aquatic ecosystems (Rosentreter et al. 2021), but field measurements are typically scarce or missing for the majority of remote areas in Africa, South America, and Asia. Consequently, the availability of low-cost portable instrumentation could help advance this research topic in regions and countries with few monitoring plans and/or where expensive instruments (portable and/or laboratory infrared/Raman spectroscopic instruments or gas chromatographs, reviewed by Kamieniak et al. 2015) are unavailable.

Here, we describe a small, low-energy, portable MOS-based methane sensor encapsulated in a hydrophobic membrane and connected to a microcontroller board with a data logger. It is well established that MOS are sensitive to humidity, temperature (van den Bossche et al. 2017) and sulfide interference (Bastviken et al. 2020). Accordingly, the tests described here were specifically designed to validate the use of submerged MOS sensors to measure methane in water.

More specifically, this communication reports a series of tests that reassemble field conditions to evaluate: (1) the lowest detection limit under controlled conditions, (2) the effect of changes in water temperature on sensor performance, and (3) dissolved sulfide interference with sensor measurements.

## Prototype and experimental design

### Prototype

We selected the methane MOS sensor TGS 2611-E00 (https://www.figarosensor.com/product/entry/tgs2611-e00.html) provided by the Figaro Company. This sensor has a conductive layer that is sensitive to the presence of volatiles and incorporates a filter that according to the product information reduces interference from volatile organics such as alcohols, rendering it more selective toward methane than other MOS sensors produced by the same company. This sensor is designed for methane detection, but the manufacturer has explicitly reported that besides methane, the sensor can also detect molecular hydrogen. Thus, although all our present results were calibrated assuming the presence of methane only, the sensor also responds to $CH_4$ and potentially interfering chemicals such as $H_2$ and sulfide (https://www.figarosensor.com/product/docs/tgs2611-e00_product%20infomation%28fusa%29_rev01.pdf). Nevertheless, in natural aquatic ecosystems, methane concentrations typically predominate over $H_2$ (Fazi et al. 2021).

We inserted the sensor into a 20 mL volume plastic flow-through vessel, through which the sample to be analyzed flowed. The sensor did not come into direct contact with the water because it was protected with a flexible hydrophobic membrane (porosity of 2 $\mu$m or less) made of extended polytetrafluoroethylene (supplied by International Polymer Engineering, product 200-07-S-X. More details at https://ipeweb.com/oem-components/co2-sensor-covers/). This approach is similar to the strategy proposed for direct measurements of $CO_2$ in water using portable NDIR sensors (Johnson et al. 2010). In addition, a low-cost, waterproof temperature sensor (DS18B20) was placed into the vessel to monitor water temperature.

The sensitive layer of the MOS sensor must be heated up to obtain an efficient chemical reaction and the sensor readout is the conductivity of the sensitive layer. The sensor was powered at 5 V by a 3.7 V (2.6 Ah) lithium-ion rechargeable battery (model ICR 18650, supplied by Samsung) coupled to a DC–DC $5 \pm 0.1$ V adjustable boost power supply with a synchronous rectifier with 96% (supplied by Great IT electronic components). The module can supply up to 1 A, which is enough to power the heater of the sensor (TGS 2600 requires a heater current of about 40 mA at 5 V). The sensor output ($V_{OUT}$) is followed by an analog signal conditioning circuit that amplifies the sensor signal 10-fold using a precision operational amplifier (OP07CP; Texas Instruments). The amplified sensor signal was sampled by means of a 16-bit analog-to-digital converter (ADC; ADS1115, supplied by Adafruit) that was configured as a single-ended input channel. Results and data analysis described below are based on $\times 10$ amplified output. The gain can be easily changed replacing the pair of resistances of the voltage amplifier Op-amp circuit. A $\times 10$ gain was selected to amplify the signal to the input range of the ADC while ensuring no signal saturation occurs. A I2C protocol was implemented on the chip to communicate and transfer acquired data. Figure 1 shows a block diagram of the signal conditioning electronics.

The sensor has a resistance ($R_S$), that decreases with increasing methane concentration. According the signal conditioning circuit, $R_S$ can be calculated by the following formula:

$$R_S = R_L\left(\frac{V_C}{V_{OUT}} - 1\right), \quad (1)$$

where $V_C$ is the supply voltage (5.0 $V_{DC}$), $V_{OUT}$ is the measured output voltage and $R_L$ is the load resistance (1 kΩ).

The selected feature to measure the methane concertation level is the ratio $R_{S(m)}/R_{S(0)}$. $R_{S(m)}$ corresponds to the lowest acquired sensor value during sample injection. $R_{S(0)}$ represents the baseline resistance, which is estimated computing the average of the 10 resistance values acquired before sample injection.

A low-cost, general purpose board was selected to acquire and store the data from the sensors (every 2.5 s). The microcontroller communicates with the analog-to-digital converter over the I2C bus and stores the readings in the SD. We used an Arduino UNO board with a XD-204 shield that incorporated an SD memory card to log the readings from the TGS and DS18B20 sensors.

The selected components were chosen for their specifications and cost-effectiveness in continuous monitoring experiments. An external computer with Arduino IDE software can be used to visualize the captured data in real-time (*see*

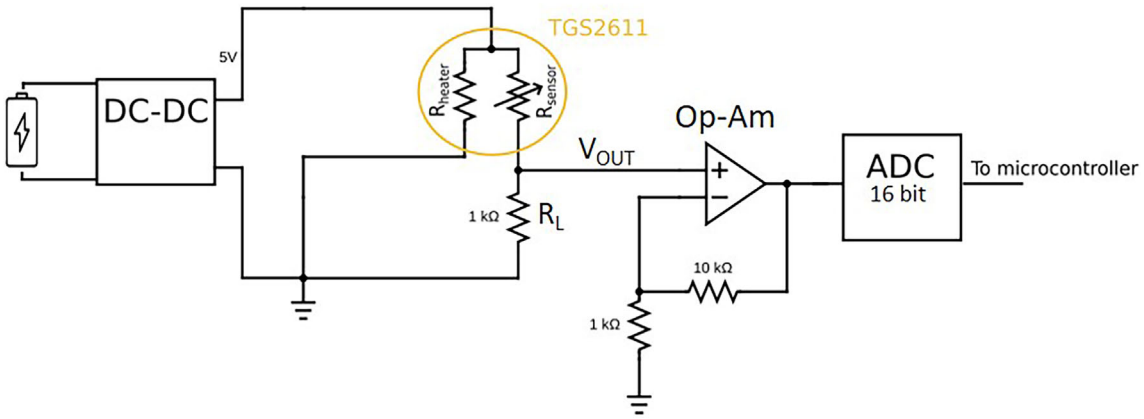


**Fig. 1.** Signal conditioning circuit for the TGS sensor. $R_L$ is the load resistance. $R_{sensor}$ is $R_S$. $V_{OUT}$ is the signal output. *See* Eq. 1 for converting $V_{OUT}$ into $R_S$. $V_{OUT}$ is amplified $\times 10$ with an operational amplifier (Op-Am) prior it is acquired by the 16 bits analog-to-digital converter (ADC).

Appendix S1 for the code created for this study). The system can be adapted to install a display on the Arduino. Table 1 lists the components used to assemble the device and their approximate cost. The total weight of the equipment is about 200 g (excluding the external computer and the 12 V battery), rendering it suitable for in situ measurements. At present, the total cost is approximately €150. If there is no need to store the data, and only readings from the TGS sensor are required, the analog-to-digital converter, the Arduino board, and the laptop can be replaced by a simple digital multimeter.

**Experimental setup and protocol**

Different methane concentrations dissolved in the sample are expected to induce different signal amplitude changes with respect to the basal level. The experimental setup included a persistaltic pump to control the sample flow rate. Control water (i.e., methane-free water) was injected continuously at a constant flow rate to set the sensor signal to basal level, and it was periodically replaced with a fixed volume of sample water (containing an unknown concentration of methane). We call this experimental approach the *flow-through* configuration (Section Flow-through configuration). During *flow-through* tests, the control samples and the measurement samples were injected at a constant rate of 0.5 mL $s^{-1}$ with a 12 V mini peristaltic pump (model G328, supplied by Grothen) into a 20 mL throw-cell. In these experiments only 40 mL of sample were injected. This sample volume was selected because is a relatively small volume that can be easily collected, transported and stored with the 60 mL plastic syringe that are frequently used for water sampling for gasses analysis. Furthermore, the volume of 40 mL doubles the throw-flow cell volume, ensuring, therefore, the complete sample injection to the cell. At the same time the approach prevents the heating of water in direct contact with the sensor into the flow-through cell and reduces the risk to generate a drift of the sensor signal.

All *flow-through* experiments started when the sensor signal reached a steady baseline. To reach this steady condition more than 2 h after plugging the sensor into the water were necessary (*see* Fig. S3 for more details).

MOS sensors are sensitive to temperature and humidity (Marco and Gutierrez-Galvez 2012). However, once the encapsulated sensor was submerged in water, moisture inside the hydrophobic membrane remained steady at 95% during measurements (*see* Fig. S4). Therefore, thanks to the configuration of the setup, cross-sensitivity to humidity is marginal, and temperature and possible interfering chemicals volatiles remain the most significant environmental variables that alter TGS sensor measurements. To evaluate the impact of temperature on sensor performance, a series of tests were performed using water temperatures of 12°C, 18.5°C, 21°C, 23.5°C, 27°C, and 28.5°C. To ensure a steady temperature, tests were performed at a stable room temperature and a laboratory water bath was used to maintain water temperatures constant. Each day, measurements corresponding to only one temperature were performed, thus simulating temperature changes across days. Stability across days can also be assessed, given that sensor drift is one of the main challenges with low-cost chemical sensors (Padilla et al. 2010; Ziyatdinov et al. 2010).

MOS based on $TiO_2$ oxide are potentially sensitive to reduced volatile molecules, despite the filter that is integrated in the TGS module. Besides the presence of methane and molecular hydrogen in anoxic water habitats, sulfate reduction respiration may release reduced volatile sulfur (i.e., sulfide $S^{2-}/H_2S$), which can coexist with methane, especially in anoxic saturated sediments (Pellerin et al. 2018) or lake bottoms (Fazi et al. 2021). We also tested sulfide interference with sensor measurements under flow-through conditions, and explored the feasibility of a simplified setup for sample injection. Therefore, to test the sensitivity of MOS to sulfide, two additional tests were performed under laboratory conditions at room temperature (24.5–25.6°C). The first test was designed to verify sensor response to a set of methane-free samples with sulfide concentrations ranging from 0 to 2 mmol $L^{-1}$. The highest sulfide concentration was in the range of that reported in sulfide-rich marine anoxic sediments

**Table 1.** Components used to assemble the device and their approximate cost.

| Item | Approx. cost (€) | Units (#) | Comment |
|---|---|---|---|
| Arduino UNO | 25 | 1 | Microcontroller board* |
| XD-204 data logger shield SD | 21 | 1 | Data logger for microcontroller board* |
| SD card | 7 | 1 | SD card with recorded data* |
| 9 V rechargeable NiMH | 15 | 1 | Power supply for microcontroller board (in the field only)* |
| 9 V battery connector | 2 | 1 | To connect 9 V battery to microcontroller board* |
| C2G USB cable | 3 | 1 | Connecting microcontroller board to PC* |
| DC–DC adjustable boost power supply (great IT electronic components) | 0.5 | 1 | 5 ± 0.1 V, 1 A power supply stabilizer |
| 3.7 V lithium-ion rechargeable battery | 9 | 2 | Power supply for methane sensor |
| TGS 2611-E00 | 20 | 1 | Methane sensor |
| DHT11 | 5 | 1 | Temperature and relative humidity sensor module |
| DS18B20 | 3 | 1 | Waterproof temperature sensor |
| Hydrophobic membrane (ePTFE) | 10 | 1 | Membrane to waterproof methane sensor |
| Set of male–female DuPont cables | 5 | 1 | Cable for connecting sensors to microcontroller board |
| OP07 operational amplifier+ resistance set | 3 | 1 | Sensor output amplification setup |
| 12 V mini peristaltic pump Grothen G328 | 10 | 1 | Peristaltic pump for flow-through measurements |
| Analog-to-Digital Converter ADS1115 module 16-Bit | 10 | 1 | To increase Arduino UNO data resolution |

Approximate total cost ~ €150.
*The elements that could be replaced with a digital multimeter if it is not necessary to save data in a file for further analysis.

(Pellerin et al. 2018) and in wastewaters (Haaning Nielsen et al. 2004). The second test was designed to explore cross-sensitivity to sulfide when methane was also present in the sample.

Finally, we also explored the feasibility of a simplified setup for the injection of the sample. The *flow-through* configuration uses a pump to control sample flow. Moreover, this configuration favors stable baseline. Therefore, we run a set of experiments without the peristaltic pump. We call this configuration discrete *pulsed* setup and the water samples were injected manually using a 60 mL syringe every 3 min. During these 3 min the injected water remains immobilized into the cell. This will cause a gradual increase of its temperature. Consequently, with the *pulsed* setup baseline changes continuously.

Both *flow-through* and *pulsed* measurements can easily be performed in situ using a 12 V battery, which can supply energy to the sensor, the electronics, and the peristaltic pump for hours. However, the *pulsed* approach might also be of interest where there is a limited energy supply and in constrained scenarios. Figure 2 shows a block diagram of the *flow-through* experimental setup, while Fig. S1 shows a picture of the experimental setup.

### Sensor calibration

We divided the acquired measurements into a calibration set and a test set. The test set included all the measurements performed in 1 d, which were all acquired at the same specific water temperature. The rest of the measurements constituted the calibration set, which we used to build a linear function that was adjusted with data from different days and water temperatures. The calibration model was then evaluated using the test set, and the mean error from the actual methane concentration and the predicted concentration from the model was computed. It is worth noting that model performance was evaluated using a double cross-validation strategy such that test data were acquired on a different day and at a different water temperature to the calibration data. This is a robust strategy that reduces risk of data overfitting and takes day-to-day variability into account in the measurements (Solórzano et al. 2018).

## Analytic methods and methane stock solution

Methane measurements from the TGS sensor were calibrated by measuring the dissolved methane concentration in the same water samples using the headspace equilibration technique (Halbedel 2015). An Agilent Technologies 7820A gas chromatograph was used to measure methane concentration in the headspace, and the result was used to estimate the methane concentration dissolved in the water samples. This is a routinely protocol adopted widely used in the literature. Twenty milliliters of water sample was degasified. The 20 mL of the water sample was vigorously mixed (with a vortex during 5 min) in the syringe of 60 mL of volume: 20 mL of water sample and 40 mL of air (the air head-space). The syringe mixing

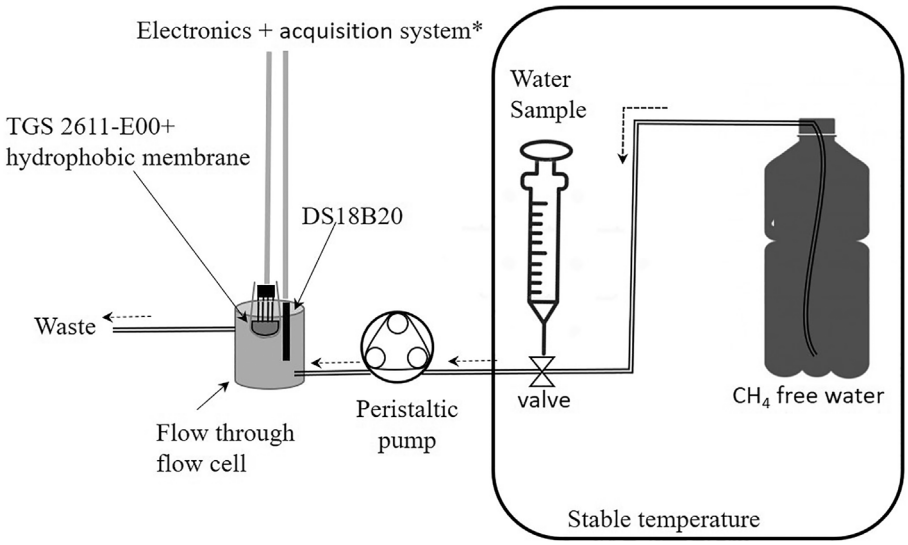


**Fig. 2.** Block diagram showing the experimental setup of the flow-through tests. **See* Fig. 1 for details on electronics and Appendix S2 for a photograph of the prototype.

allows the gas equilibrium between the head-space air and water into the syringe. Successively 15 mL of head-space air were inserted into a glass vacutainer and then inserted to the GC. Gas concentration measured in the head-space air with GC is converted into gas concentration in water considering temperature, water, and air volumes in the syringe and methane solubility in water (for further details *see* Sander 2015).

Due to the potential effect of volatile sulfide interference with the sensor response, the sulfide concentration in waters was measured manually during tests using the colorimetric method described by Pachmayr (1960).

Dissolved methane for injection into the test vessel was obtained from a stock solution consisting of distilled water (nitrate- and sulfate-free) that saturated an organic rich compost stored in an hermetic glass jar that was kept in the dark and under anoxic conditions at 25°C for more than 1 month. This natural reactor stimulated the progressive accumulation of biogenic methane in the interstitial water. The dissolved methane concentration in the jar was typically higher than 300 $\mu$mol $L^{-1}$. The stock solution was then used to prepare water samples with methane concentrations ranging from 0.10 to 5 $\mu$mol $L^{-1}$. The samples (60 mL in a plastic syringe) were prepared immediately prior to injection into the vessel.

## Results

### Flow-through configuration

#### *Temperature dependency*

Each *flow-through* test consisted of continuous injection of the control water (i.e., distilled water) into the vessel, at a constant flow rate and a fixed temperature. Between four and six water samples with different methane concentrations were injected at different time intervals using a 60 mL plastic syringe connected to a peristaltic pump. Forty milliliters of each water sample was injected, while the remaining 20 mL was used to measure methane concentration via gas chromatography and thus obtain a calibration curve between sensor response (peak amplitude) and the measured methane concentrations. Figure 3 shows the results of a test performed at 27°C, which consisted of injecting five samples with a methane concentration ranging between 0.15 and 0.9 $\mu$mol $L^{-1}$. In flow-through tests, the response of the sensor resistance $R_S$ followed a clear pulse shape. Peaks ($R_{S(m)}$, Eq. 1) were usually detected after 100–110 s after the sample injection and the sensor signal typically takes about 8–10 min to return to the baseline level.

The sample injection protocol adopted in these tests prevents to reach the signal plateau response. Preliminary long-term injection tests revealed that plateau conditions were typically obtained 2.5 min after sample addition (Fig. S4). However, during flow-through experiments the sensor signal change was abrupt and the time to reach the 90% of the signal peak typically lasted 80–90 s. Therefore, during the flow-through tests the observed signal peaks should be in between the 90% and 100% of the corresponding plateau.

Figure 3 also shows that water temperature was nearly steady during tests. However mild temperature shifts (typically < 0.3°C) were detected at the beginning of each sample injection.

In these experiments, sulfide concentrations in all samples were lower than 15 $\mu$mol $L^{-1}$ (*see* Section Pulse flow tests, sulfide interference with sensor measurements).

Figure 4 shows the relationships between measured methane and sensor responses during the tests performed at different water temperatures. In all tests, we observed a linear relationship between methane concentration and sensor response. We also found that at between 18°C and 29°C, sensor sensitivity was independent of water temperature, but the experiment

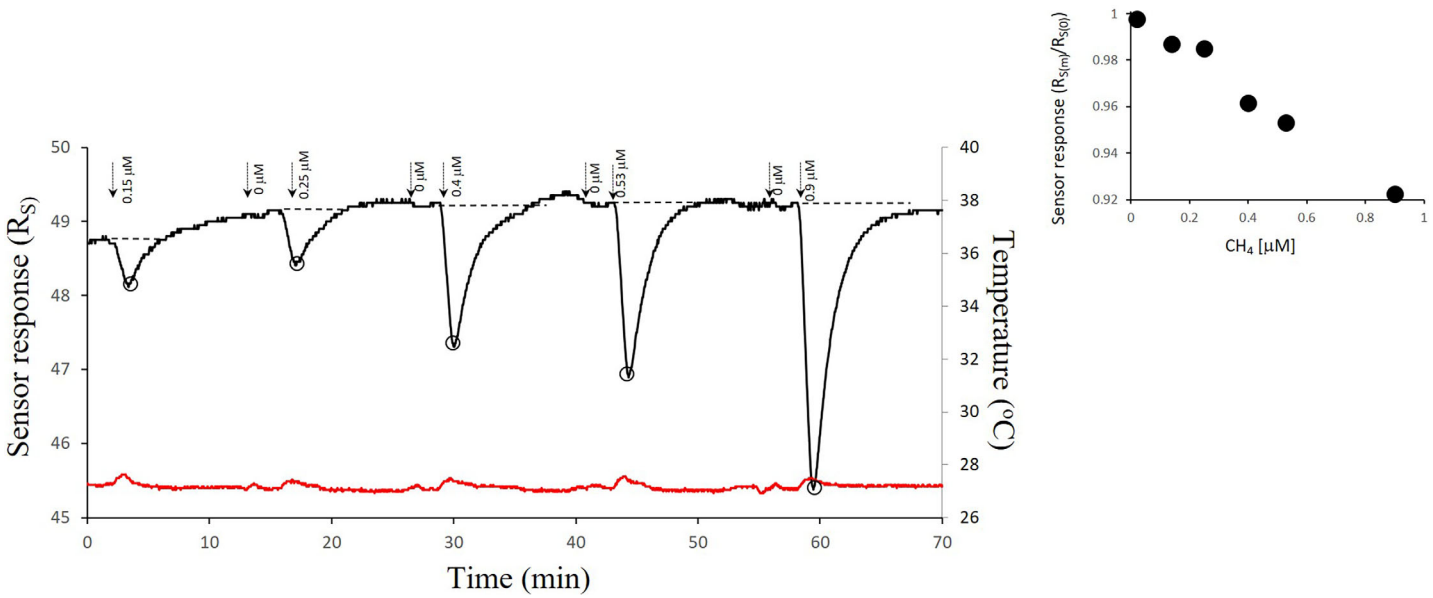


**Fig. 3.** Flow-through test. Example of sensor response (black line) after controlled injection of five samples with a methane concentration ranging from 0.15 to 0.9 mmol $L^{-1}$. Each injection was preceded by the injection of a methane-free sample. This test was performed at 27°C (red line). Vertical arrows indicate timing of sample injections. The dashed horizontal black line shows the baseline signal ($R_{S(0)}$). The black circles indicate the $R_{S(m)}$ value for each sample (*see* Eq. 1 for more details). Inset on the right shows the relationship between methane concentrations (estimated with gas chromatography) vs. peak amplitude $R_S/R_0$.

performed at 12°C revealed a significant decrease in sensor sensitivity with respect to sensor behavior above this temperature.

### *Calibration model*

We built calibration models using the data acquired in the temperature range of 18.5–29°C; measurements performed at 12°C were not considered given the variation observed in sensor behavior (*see* Fig. 3).

Figure 5 shows the model built with temperatures (ranging from 21°C to 28°C) that were acquired on four different days, and the test measurements used to evaluate the calibration model, which were acquired at a water temperature of 18.5°C on another day. The sensor sensitivity obtained for this particular model was $P = -0.089$ $(\Omega/\Omega)/\mu$mol $L^{-1}$.

This process was repeated until all the days were used to evaluate the model (mean of the error across all the repetition

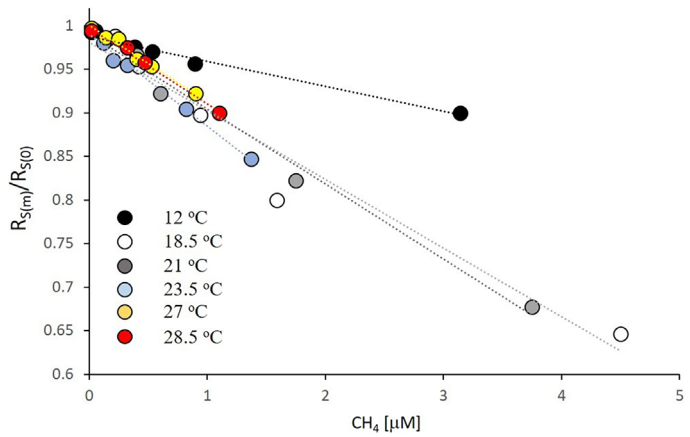


**Fig. 4.** Relationship between sensor responses ($R_{S(m)}/R_{S(0)}$) and methane concentrations in the six flowthrough tests performed at different water temperatures. Dashed lines show the regression model for each test (all models were $p < 0.01$).

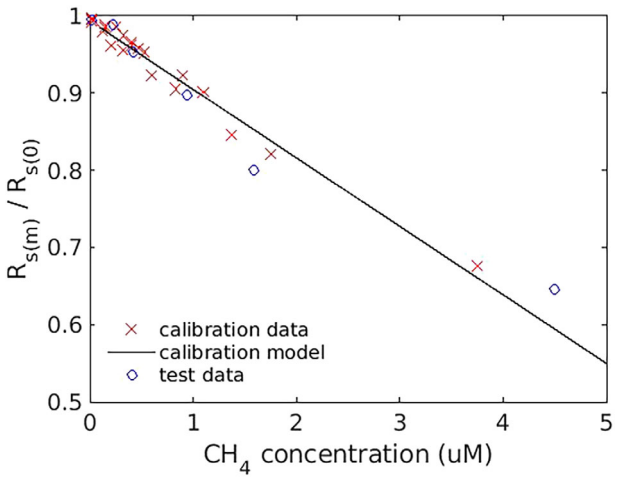


**Fig. 5.** Calibration model (black line) built with calibration data (red marks) from data acquired on 4 d at different water temperatures (21°C, 23°C, 27°C, and 28°C). The model was evaluated using test data (blue marks) acquired on a different day and at a water temperature of 18.5°C.

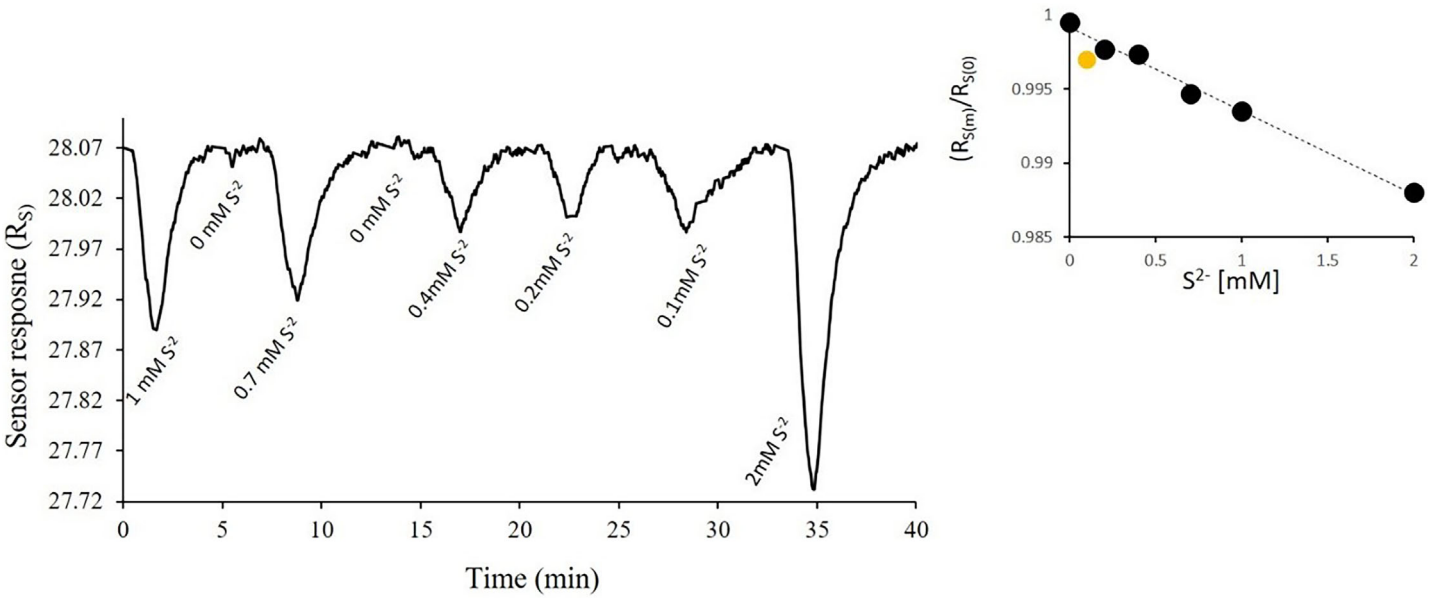


**Fig. 6.** Temporal dynamic of sensor signal following injection of methane-free water samples with different sulfide concentrations. The inset shows the sulfide concentration vs. sensor signal variation plot. The orange dot in the inset was considered an outlier in the regression analysis (dotted line, $r^2 = 0.98$, df = 4, $p < 0.01$).

is 0.085 $\mu$mol $L^{-1}$). We therefore conclude that our system, in a flow-through configuration, is capable of predicting the concentration of methane with an error of 0.085 $\mu$mol $L^{-1}$, provided that water temperature is in the range 18.5–28°C.

### Cross-sensitivity to sulfide

The measurements performed to evaluate the cross-sensitivity to sulfide were carried out with methane-free samples at room temperature with sulfide concentrations ranging from 0 to 2 mmol $L^{-1}$. The results showed that the MOS sensor was sensitive to sulfide in aquatic environments at sulfide concentrations in the presented range of sulfide concentration, indicating that sulfide interferes with methane measurements (*see* Fig. 6).

We then built a calibration model based on the experiments performed at different sulfide concentrations with no methane (*see* Fig. 7) and computed sensor cross-sensitivity to sulfide, obtaining a sensitivity of −0.006 (Ω/Ω)/mmol $L^{-1}$. Note that sensor sensitivity to sulfide was about 14,000 times lower than sensor sensitivity to methane when only one of the chemicals was present in the sample.

The next set of measurements were performed with water samples with sulfide and methane. Figure 8 shows output from a test that consisted of injecting three water samples contaminated with 0.8 mmol $L^{-1}$ of sulfide and containing methane concentrations of 1.8, 0.8, and 0.1 $\mu$mol $L^{-1}$, respectively. Sulfide interference was more marked with low methane concentrations. Comparing the signal peaks with those obtained from samples containing an identical methane concentration but no sulfide, we found that under the experimental condition, sulfide interference was marginal in samples with a methane concentration higher than 0.8 $\mu$mol $L^{-1}$. However, at methane concentrations in the range of 0.1–0.3 $\mu$mol $L^{-1}$ (i.e., at the limit of sensor performance), a sulfide concentration of 0.8 mmol $L^{-1}$ almost duplicated the sensor response when compared with sulfide-free samples. This result was confirmed by the sensor sensitivities encountered in the previous section. A sulfide concentration of 0.8 mmol $L^{-1}$ is expected to induce a signal amplitude of 8.4 mV. Similarly, 0.1 $\mu$mol $L^{-1}$ of methane will result in a sensor output of 8.9 mV. Therefore, assuming a simple additive sensor response, in the absence of sulfide or with the addition of 0.8 mmol $L^{-1}$ of sulfide, the same methane concentration of 0.1 $\mu$mol $L^{-1}$ is expected to increase by a factor of 2. Specifically,

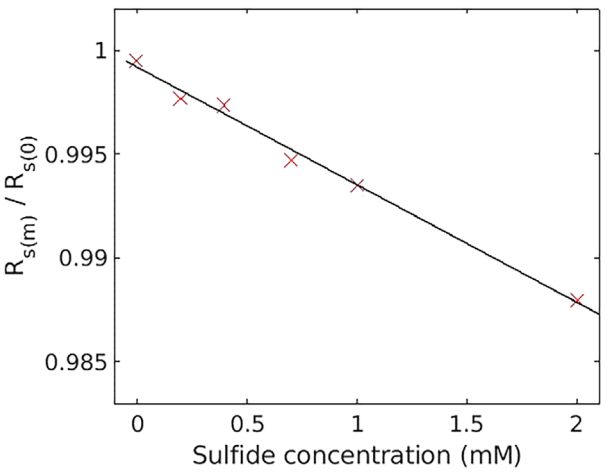


**Fig. 7.** Sensor response under different sulfide concentrations in methane-free water samples.

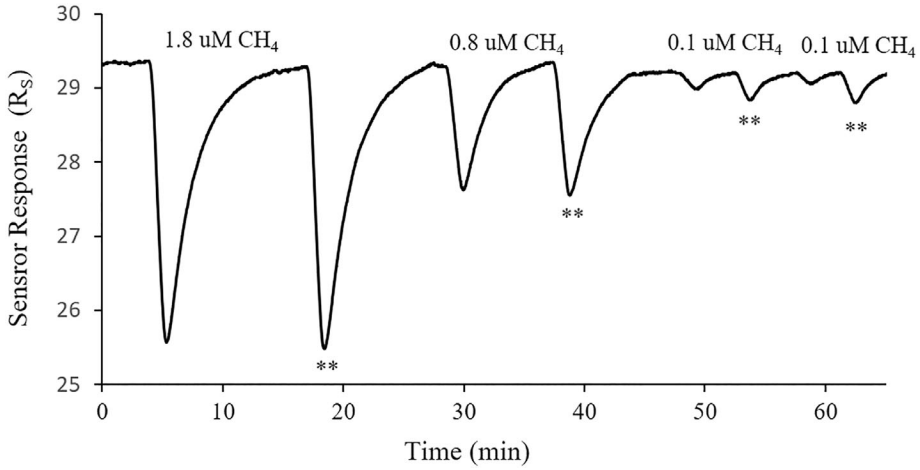


**Fig. 8.** Temporal dynamic of sensor signal following injection of water samples with different methane concentrations. Asterisks indicate peaks from samples contaminated with 0.8 mmol $L^{-1}$ of sulfide.

for the example presented here, the estimated methane would be 0.2 $\mu$mol $L^{-1}$ if sulfide interference was not taken into account.

### Pulse flow tests

The previous section described *flow-through* experiments, where the continuous flow of water through the vessel rendered it possible to maintain a relatively steady water temperature in the vessel during tests and a nearly steady baseline. However, is it possible to perform viable measurements under less strict water temperature and baseline conditions? This approach might be of interest when performing in situ measurements without a peristaltic pump and/or with a limited energy supply.

Figure 9 shows a test that consisted of manually injecting 40 mL of water sample every 3 min. In this example, the water temperature was initially set at 28°C, but it increased gradually to 28.5°C after 3 min in the vessel. As a result, although the water temperature was not steady, it displayed a controlled, repetitive baseline pulse pattern that reflected the periodic input of new water. In this test, five samples with methane concentrations ranging between 0.15 and 1.73 $\mu$mol $L^{-1}$ were injected between distilled water samples. The results showed that the sensor signal baseline pulse pattern, was temporarily interrupted by the inputs of samples with a methane concentration higher than 0.35 $\mu$mol $L^{-1}$. In contrast, samples with a methane concentration lower than 0.2 $\mu$mol $L^{-1}$ did not

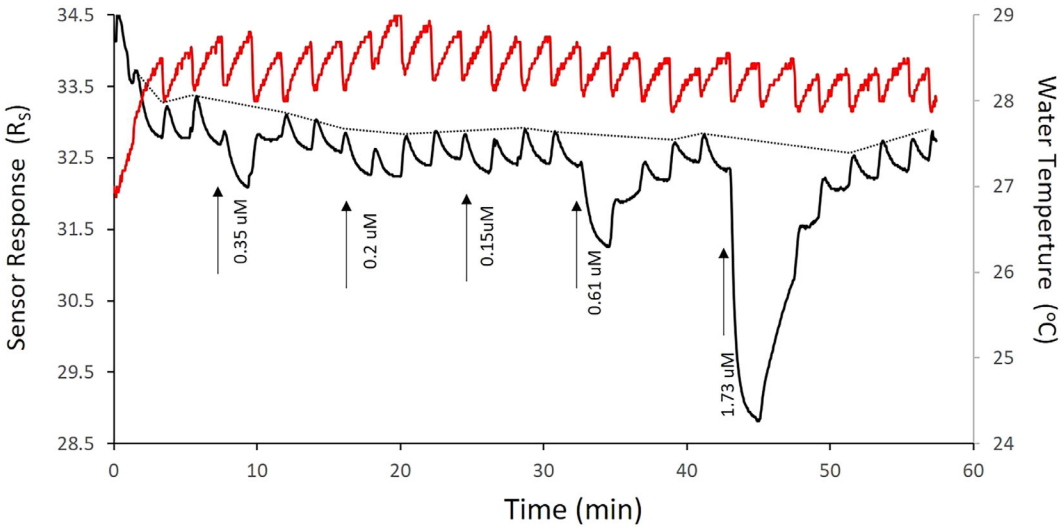


**Fig. 9.** Example of a pulse flow test. Sensor response (black line) during a calibration experiment that consisted of injecting 27 samples (40 mL each) every 3 min. Of 27 samples, 5 contained methane concentrations ranging from 0.15 to 1.73 mmol $L^{-1}$. The remaining samples were distilled water and helped to return the signal to basal level and to calculate $R_0$ (dashed black line). Water temperature (red line) showed a periodic pattern (between 28°C and 28.5°C) that reflected the sequential input of new water and the impact of the sensor in modifying the water temperature into the flow-through cell. Arrows indicate the timing of five samples injection.

produce a sensor signal that differed from that of baseline. Moreover, the pulse dynamic of the sensor signal rendered it more difficult to identify the basal line and thus to estimate the height of peaks. In summary, although the pulse test made it possible to optimize the equipment (removing the peristaltic pump and saving energy), sensor sensitivity was lower than that observed with flow-through tests. However, this example shows that in some circumstances (i.e., energy supply limitations, failure of the peristaltic pump), different strategies can be used to perform preliminary measurements.

## Discussion and conclusions

We have presented a low-cost system for measuring methane dissolved in water samples using a MOS sensor. The sensor is covered with a hydrophobic membrane that enables the sensor to be submerged in water. Our measurements show that the system presents a stable response provided that the water temperature is in the range of 18.5–28°C. A calibration model was built using measurements obtained on different days and evaluated with data acquired on another day. The prediction error for new measurements was estimated at 0.06 $\mu$mol $L^{-1}$, in the measurement range from 0.1 to 4.5 $\mu$mol $L^{-1}$ of methane in water.

Dissolved methane concentrations in aquatic ecosystems vary widely from a few nmol $L^{-1}$ to more than 100 $\mu$mol $L^{-1}$ (Fazi et al. 2021), with concentrations in saw grass, forest swamps, lakes, and the hypolimnion typically being higher than 1 $\mu$mol $L^{-1}$ (Barber et al. 1988). Moreover, concentrations in anoxic aquatic habitats such as the bottom waters of meromictic lakes, interstitial sediments, and artificial aquatic systems (i.e., residual water treatment plants for rice fields) are even higher (Daelman et al. 2012). Consequently, this report confirms that submerged MOS sensors may provide rapid, cheap, and valuable information about the abundance of dissolved methane in most of these aquatic ecosystems.

Calibration with measurements from a reference instrument is mandatory. Moreover, interference from other reduced molecules (i.e., sulfide) must be evaluated carefully. From a more pragmatic perspective, the most critical aspect is to control the water temperature during measurements. Our tests evidenced that the temperature itself is not an obstacle, but it is crucial that the control water and the water samples are at the same temperature. In the laboratory, it is easy to maintain control water and samples at the same temperature, but in the field, this is more difficult to accomplish. However, a low-cost solution can be adopted. The most usual situation is probably that the temperature of the control water is higher than that of samples, and in this case, it is sufficient to cool the control water down to the desired temperature by adding crushed ice from a cooler. The opposite situation is probably more unusual, but in this case, the control water can be heated by adding hot water from a thermos. For in situ measurements, the control water should be transported in a tank. Our flow-through tests consumed almost 2 L $h^{-1}$, indicating that a 20 L tank would be necessary for 2–3 h to get the baseline and 6 h of measurements. Nevertheless, we have also proposed a pulsed configuration that halves the required water volume.

The impact of environmental temperature on MOS sensor performance is well known (Huerta et al. 2016; Abdullah et al. 2020). Our tests evidenced that sensor sensitivity remained relatively steady at water temperatures between 18°C and 30°C. We built a calibration model considering this range of temperatures. Nevertheless, the model could be extended to a wider range of temperatures if the prediction accuracy requirements are relaxed. If the system demands higher sensitivity, we would recommend injecting a large volume of sample water or/and reducing the flow of the peristaltic pump.

With respect to interference of sulfite, our tests revealed that to prevent any overestimation of methane concentration, in samples with a low methane content (e.g., <0.5 mol $L^{-1}$) and high sulfide interference, it is essential to determine the concentration of sulfide to correct cross-sensitivity. In this context it is also important to remark that sulfide is extremely corrosive: we observed that high sulfide concentrations irremediably damage the sensor in a short time. In consequence we discourage the implement of this sensor in anoxic aquatic habitats with high sulphate concentrations, such as gypsum rich hypersaline lagoons, where sulfate reduction/sulfide production rates are usually extremely high. Under these conditions, the sensor performance may deteriorate very rapidly.

In summary, MOS technology offers the possibility of designing studies that would otherwise be unaffordable using more expensive technology. In terms of methane concentrations, for example, it costs less than €150 to set up a small, simple, portable system for measuring dissolved methane in water. But this could simply be the first step.

For instance, it would be easy and inexpensive to assemble an arrangement of "*n*" sensors for online monitoring. For instance, it exists an enormous interest in measuring methane production in bioreactors in the context of biocombustible production research. Evidently these studies might strongly benefit from online continuous methane measurements. A low-cost microcontroller coupled with an Analog-to-Digital Converter ADS 1115 module can register data from up to four sensors. An array of such sensors plus an Arduino board (or other open source electronic microprocessor) might cost €300, including all the electronics and pneumatic equipment, rendering continuous multiple online methane measurements in the field or in the laboratory affordable because the risk–benefit ratio is severely reduced.

**Data availability statement**

The data that support the findings of this study are available on request from the authors.

## *References*


Abdullah, A. N., K. Kamarudin, S. M. Mamduh, A. H. Adom, and Z. H. M. Juffry. 2020. Effect of environmental temperature and humidity on different metal oxide gas sensors at various gas concentration levels. IOP Conf. Ser.: Mater. Sci. Eng. **864**: 012152. doi:10.1088/1757-899X/864/1/012152

Barber, T. R., R. A. Burke Jr, and W. M. Sackett. 1988. Diffusive flux of methane from warm wetlands. Glob. Biogeochem. Cycles **2**: 411–425. doi:10.1029/GB002i004p00411

Bastviken, D., J. Nygren, J. Schenk, R. Parellada Massana, and N. T. Duc. 2020. Facilitating the use of low-cost methane ($CH_4$) sensors in flux chambers–calibration, data processing, and an open-source make-it-yourself logger. Biogeosciences **17**: 3659–3667. doi:10.5194/bg-17-3659-2020

Daelman, M. R., and others. 2012. Methane emission during municipal wastewater treatment. Water Res. **46**: 3657–3670. doi:10.1016/j.watres.2012.04.024

Eugster, W., and G. W. Kling. 2012. Performance of a low-cost methane sensor for ambient concentration measurements in preliminary studies. Atmos. Meas. Tech. **5**: 1925–1934. doi:10.5194/amt-5-1925-2012

Fazi, S., and others. 2021. High concentrations of dissolved biogenic methane associated with cyanobacterial blooms in East African lake surface water. Commun. Biol. **4**: 845. doi:10.1038/s42003-021-02365-x

Haaning Nielsen, A., J. Vollertsen, and T. Hvitved-Jacobsen. 2004. Chemical sulfide oxidation of wastewater-effects of pH and temperature. Water Sci. Technol. **50**: 185–192. doi:10.2166/wst.2004.0258

Halbedel, S. 2015. Protocol for CO2 sampling in waters by the use of the headspace equilibration technique, based on the simple gas equation; second update. Protoc. Exch. doi:10.1038/protex.2015.085

Huerta, R., T. Mosqueiro, J. Fonollosa, N. F. Rulkov, and I. Rodriguez-Lujan. 2016. Online decorrelation of humidity and temperature in chemical sensors for continuous monitoring. Chemom. Intell. Lab. Syst. **157**: 169–176. doi:10.1016/j.chemolab.2016.07.004

Johnson, M. S., M. F. Billett, K. J. Dinsmore, M. Wallin, K. E. Dyson, and R. S. Jassal. 2010. Direct and continuous measurement of dissolved carbon dioxide in freshwater aquatic systems—Method and applications. Ecohydrology **3**: 68–78. doi:10.1002/eco.95

Jørgensen, C. J., J. Mønster, K. Fuglsang, and J. R. Christiansen. 2020. Continuous methane concentration measurements at the Greenland ice sheet–atmosphere interface using a low-cost, low-power metal oxide sensor system. Atmos. Meas. Tech. **13**: 3319–3328. doi:10.5194/amt-13-3319-2020

Kamieniak, J., E. P. Randviir, and C. E. Banks. 2015. The latest developments in the analytical sensing of methane. TrAC Trends Anal. Chem. **73**: 146–157. doi:10.1016/j.trac.2015.04.030

Marco, S., and A. Gutierrez-Galvez. 2012. Signal and data processing for machine olfaction and chemical sensing: A review. IEEE Sens. J. **12**: 3189–3214. doi:10.1109/JSEN.2012.2192920

Pachmayr, F. 1960. Vorkommen und Bestimmung von Schwefelverbindungen in Mineralwasser. Ph.D. thesis. Universitat Munchen.

Padilla, M., A. Perera, I. Montoliu, A. Chaudry, K. Persaud, and S. Marco. 2010. Drift compensation of gas sensor array data by orthogonal signal correction. Chemom. Intell. Lab. Syst. **100**: 28–35. doi:10.1016/j.chemolab.2009.10.002

Pellerin, A., and others. 2018. The sulfur cycle below the sulfate-methane transition of marine sediments. Geochim. Cosmochim. Acta **23**: 74–89. doi:10.1016/j.gca.2018.07.027

Rosentreter, J. A., A. V. Borges, B. R. Deemer, M. A. Holgerson, S. Liu, C. Song, and B. D. Eyre. 2021. Half of global methane emissions come from highly variable aquatic ecosystem sources. Nat. Geosci. **14**: 225–230. doi:10.1038/s41561-021-00715-2

Sander, R. 2015. Compilation of Henry's law constants (version 4.0) for water as solvent. Atmos. Chem. Phys. **15**: 4399–4981. doi:10.5194/acp-15-4399-2015

Saunois, M., A. R. Stavert, B. Poulter, P. Bousquet, J. G. Canadell, R. B. Jackson, and Q. Zhuang. 2020. The global methane budget 2000–2017. Earth Sys. Sci. Data **12**: 1561–1623. doi:10.5194/essd-12-1561-2020

Solórzano, A., R. Rodríguez-Pérez, M. Padilla, T. Graunke, L. Fernandez, S. Marco, and J. Fonollosa. 2018. Multi-unit calibration rejects inherent device variability of chemical sensor arrays. Sens. Actuators B: Chem. **265**: 142–154. doi:10.1016/j.snb.2018.02.188

van den Bossche, M., N. T. Rose, and S. F. J. De Wekker. 2017. Potential of a low-cost gas sensor for atmospheric methane monitoring. Sens. Actuators B: Chem. **238**: 501–509. doi:10.1016/j.snb.2016.07.092

Ziyatdinov, A., S. Marco, A. Chaudry, K. Persaud, P. Caminal, and A. Perera. 2010. Drift compensation of gas sensor array data by common principal component analysis. Sens. Actuators B: Chem. **146**: 460–465. doi:10.1016/j.snb.2009.11.034



**Acknowledgments**

This study was funded by MCIN/AEI/10.13039/501100011033 (projects RTI2018-097950-B-C21, PID2021-123735OB-C22, and TEC2014-60337-R, DPI2017-89827-R) and ACCIÓ (Innotec ACE014/20/000018, Generalitat de Catalunya). We acknowledge CERCA Programme / Generalitat de Catalunya. We also thank the Networking Biomedical Research Centre in the subject area of Bioengineering, Biomaterials and Nanomedicine (CIBER-BBN), initiatives of Instituto de

Investigación Carlos III (ISCIII), and Share4Rare project (Grant Agreement 780262). B2SLab is certified SGR 952. AB is a member of the SGR 976. JF acknowledges the support from the Serra Húnter program. We thank Ariadna Vidal for helping with experiments and Jordi Pastor (CCiTUB) for helping in assembling an initial prototype. Finally, we want to thank the two anonymous reviewers for their constructive suggestions and contributions during the review process.

*Submitted 15 February 2022*
*Revised 26 August 2022*
*Accepted 31 August 2022*

*Associate editor: Mike DeGrandpre*